

The Influence of Pyrolysis on Physical Properties and Microstructure of Modified PAN Fibers during Carbonization

TSE-HAO KO

Department of Materials Science, College of Science, Feng Chia University, Taichung, Taiwan, Republic of China

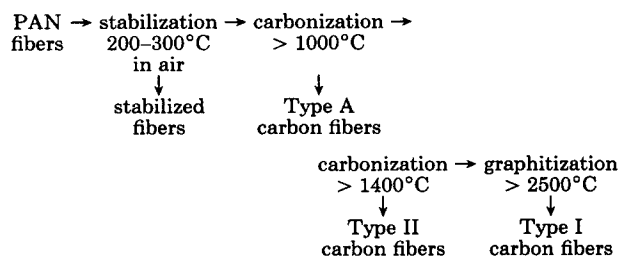
SYNOPSIS

Modification of polyacrylonitrile (PAN) fibers with potassium permanganate has reduced the time required for stabilization and also improved the mechanical properties of the resulting carbon fibers. In this study, the effect of modification on the physical properties, microstructure, and elemental composition of fibers during the carbonization process was examined for the first time. The resulting carbon fibers developed from modified PAN fibers had a higher density, a greater stacking size (L_c), and a higher preferred orientation than those developed from unmodified PAN fibers. The carbon fibers developed from the modified PAN fibers also showed an improvement in tensile strength from 20 to 40%. These fibers showed a radial structure in the fracture surface and were somewhat different structurally in the cross section than were the carbon fibers developed from the original PAN fibers. A model for the structure of both carbon fibers is presented. The relationship between the formation of closed pores from open pores and the variety of cumulative pore area during the heat-treatment stage is also discussed.

INTRODUCTION

Carbon fibers have been known as filaments for lamps for nearly a century, since Edison first used them.¹ Modern carbon fibers were first developed by Shindo² in 1961 when he pyrolysed polyacrylonitrile (PAN) fiber. Following this discovery by Shindo, the development of commercial carbon fibers was reported by Watt and co-workers.³ Typically, the PAN fibers are stabilized in air at 200–300°C and carbonized in an inert gas up to 1000°C. This process produces Type A carbon fibers with a low modulus and a low tensile strength. PAN fibers can also be carbonized at up to 1400°C to produce Type II carbon fibers, exhibiting high tensile strength and medium modulus. Graphitization, which occurs in heat treatment at temperatures higher than 2500°C to make Type I carbon fibers, can also be used to increase the modulus. This process, however, often decreases the tensile strength. A flow chart repre-

senting the manufacture of carbon fibers from PAN fibers presented the following⁴:



Carbon fibers are now extensively used in resin composite systems and even metals to yield composite materials of high specific stiffness, strength, and light weight. The materials are now important industrially and have gained a wide range of application from game and sports articles to the aerospace industry. Because of their various technological applications in the industrial and engineering fields, the development of high-strain and high-modulus carbon fibers has become necessary. The trends in research and development of PAN-based carbon fibers may be classified as follows⁵:

1. Increase the allowable design strain and impact resistance to produce high-strength and high-strain fibers.
2. Increase the high modulus, especially in space applications.
3. Produce a high modulus with high strength, in the same fiber, which is especially important in aerospace application.

The best method for obtaining high-strain carbon fiber is to improve fiber strength. It has been established that the treatment of a PAN fiber under a tension load improves the fiber quality.^{6,7} Mathur et al.⁸ and Bahl et al.^{9,10} have pretreated a PAN fiber with CuCl to make high-performance carbon fibers. Cagliostro¹¹ has modified a PAN fiber with benzoic acid to improve carbon fiber strength.

Two previous studies^{12,13} presented the results of our process for modifying the PAN fibers with potassium permanganate to produce high-performance carbon fibers. We have discussed the reasons why a PAN fiber modified with potassium permanganate can reduce stabilization time and improve the mechanical properties of the carbon fiber.¹⁴ In another study,¹⁵ we investigated the morphology and microstructure of a stabilized fiber, using optical and electron microscopes. We presented a model for the structure of the stabilized fibers. We have done an additional study on the effect of modification on the stabilization process and the dynamic mechanical properties of PAN fibers.¹⁶ Earlier, we also reported on the variation of crystal size in PAN fibers during stabilization. We provided a model of the ladder polymer in stabilized fibers transformed from acrylonitrile (AN) units of PAN fiber.¹⁷

The present report is concerned with the variation of physical properties and microstructural changes in two different kinds of stabilized fibers: One was developed from PAN fibers and the other developed from modified PAN fibers. The progression of the carbonization process used for both kinds of fibers was analyzed through measurements of mechanical properties, density, elemental composition, microstructure parameters, and pore-size distribution. This study provides a sound basis for understanding how the modification of PAN fibers can produce a higher-quality and higher tensile strength carbon fibers than was previously possible.

EXPERIMENTAL

Materials

A special grade of polyacrylonitrile (PAN) fiber tows (Courtelle fiber, Courtaulds Ltd., U.K.), containing

6% methyl acrylate and about 1% (itaconic) acid copolymer, was used in this study. Each single tow of this fiber contained 6000 filaments of 1.1 denier. PAN fibers were modified with hot potassium permanganate solution at 85°C for 2 min, with a fixed-length method. The color changed from clear white to brown after the modification. This sample was washed with distilled water and dried to a constant weight in an oven. The manganese content in the prepared carbon fibers was determined by atomic emission spectroscopy and was found to have increased about 60 times over its original content.¹³

Stabilization and Carbonization

The stabilization of the PAN fibers and the modified PAN precursors was carried out in a constant temperature-zone furnace, with a fixed-length method, at 230°C for 60 min in a purified air atmosphere. The stabilized fibers were named fibers A and B, respectively. The properties of fibers A and B will be discussed further in the following section. The stabilized fibers (fibers A and B) were carbonized to 1300°C at a rate of 240°C/h from 25 to 1300°C in a ceramic reaction tube and an oxygen-free nitrogen atmosphere, respectively. Neither tension nor load were applied to the fibers during this process. The samples were heated in this way at different temperatures from 300 to 1300°C, at 100°C intervals.

Mechanical Properties

The mechanical properties of the fibers were determined according to JIS R7601-1980 testing methods with the Instron Universal Testing Machine at a crosshead speed of 0.5 mm/min, a load cell of 20 g, and 2.5 cm of testing gauge. In each specimen, at least 25 filaments were tested. Their average value is reported here.

Wide-Angle X-Ray Diffraction

A Rigaku X-ray diffractometer, providing Ni-filtered CuK α radiation, was used to measure the crystalline-related properties of the sample. The step-scan method was used to determine the d spacing and stacking size (L_c , stacking height of layer planes). The step-interval was set at 0.02°. The preferred orientation of the carbon fibers $O(002)$ was determined by an X-ray diffractometer, with a fiber specimen attachment. The precursors were located at around 25° (2θ). [The (002) plane of carbon fibers is thought to have a hexagonal structure.] The 360° azimuthal circle was used in order to permit the fiber

axis to be rotated 360° around the vertical. The d spacing, L_c , and $O(002)$ were calculated by using eqs. (1) (the Bragg equation), (2) (the Scherrer equation), and (3), respectively:

$$n\lambda = 2d \sin\theta \quad (1)$$

$$L(hkl) \text{ (in nm unit)} = K\lambda/B \cos\theta \quad (2)$$

$$O(hkl) \text{ (in \%)} = [(360 - H)/360]100 \quad (3)$$

in which $\lambda = 0.154$ nm, K is the apparatus constant ($= 1.0$), and B is the half-value width in the radian of the X-ray diffraction intensity (I) vs. 2θ curve. H is the half-value width in degrees of the curve of (I) vs. azimuthal angle.¹⁶ The preferred orientation, $O(002)$, has a value of 0 if the specimen is completely unoriented. If the crystallites are all arranged perfectly parallel to one another, the preferred orientation is equal to 100.

Density

Densities were measured at 25°C according to the density gradient column method. The density column was prepared with a mixture of *n*-heptane and carbon tetrachloride, so that a density gradient of about 1.2–1.6 g/cm³ extended from top to bottom. For the measurement of densities from 1.6 to 2.0 g/cm³, a density gradient column prepared with a mixture of carbon tetrachloride and 1,3-dibromopropan was adopted.

Elemental Analysis

Elemental analysis was carried out with a Perkin-Elmer model 240C elemental analyser. The samples from the carbonization process were analyzed for carbon, hydrogen, and nitrogen. The oxygen content was determined by the difference between these three.

Pore-Size Distribution

Mercury porosimetry of all samples was carried out with a Micromeritics mercury porosimeter pore-size

Table I Properties of Stabilized Fibers Used

Sample	Developed from	Strength (GPa)	Modulus (GPa)	Density (g/cm ³)	AI* (%)
Fiber A	PAN fiber	0.28	1.34	1.342	49.6
Fiber B	Modified PAN fiber	0.34	1.45	1.340	44.5

* Aromatization index (AI) was tested by a wide-angle X-ray diffractometer.¹³

Table II The Elemental Contents of Stabilized Fibers

Sample	Element Contents (wt %)			
	C	N	H	O
Fiber A	60.1	21.4	4.0	14.5
Fiber B	60.4	21.6	4.1	13.9

analyzer Model II 9220, working up to 60,000 psi, equivalent to a pore size ranging from 3.0 to 100,000 nm diameter.

Scanning Electron Microscope (SEM)

The fracture surfaces of carbon fibers were examined with a scanning electron microscope, Hitachi model S-520, at 25 KV accelerating potential. The specimens were coated with Au to get a better image.

RESULTS AND DISCUSSION

Properties of Samples

Two different stabilized fibers were used. Fiber A was developed from PAN fiber, and fiber B, from modified PAN fiber. The properties and elemental contents of the fibers before carbonization are given in Tables I and II.

Tables I and II show that fiber A has a lower strength, a higher aromatization index (AI) value, and a greater oxygen content than does fiber B. When PAN fiber is heated at above 180°C in the presence of oxygen, C≡N bonds will be converted into C=N bonds, the ladder polymer will be formed, and the cohesive energy between the relative chains will drop appreciably.^{18,19} This drop accounts for the decrease in tensile strength of the stabilized fibers. The percentage conversion of C≡N to the C=N group depends on the extent of stabilization. A higher percentage conversion (a higher AI value), indicates that stabilized fibers have more ladder polymer. Therefore, the strength is lower for fiber A than for fiber B.

The analysis of the elemental contents of the stabilized fibers is shown in Table II. The oxygen content for fiber A is higher than that for fiber B. It was found that oxygen is introduced in the form of OH and C=O groups and bonded to the carbon backbone of the ladder polymers.²⁰ Watt¹⁸ found that most of the oxygen of C=O is released as water vapor during carbonization. The carbonization process produces a cross-linking between adjacent

chains. Bahl and Manocha²¹ indicated that this cross-linking obtained by carbonizing the stabilized fiber accounts for the increase in the strength of carbon fibers.

The densities of stabilized fibers are due to the structural rearrangements associated with the cyclization reactions and the incorporation of oxygen. Fiber A shows high-density values, which suggests a high rate of stabilization in this fiber. Because fiber A has more ladder polymers, a higher oxygen content, and a higher density than does fiber B, it may seem reasonable to assume that the strength of the resulting carbon fibers developed from fiber A is greater than that developed from fiber B. However, the properties of the resulting carbon fibers proved to be exactly the opposite of those expected. The reasons for these findings are discussed in the next sections.

Elemental Analysis of Fibers during Carbonization Stage

There is a large weight loss during carbonization, producing a large volume of volatile gases and some tarry substances. Volatile compounds such as HCN, H₂, NH₃, CO₂, CO, and CH₄ are formed. Several authors studied the volatile products evolved during carbonization and have tried to deduce the chemical processes that occurred.^{4,22,23} In most cases, gas evolution was observed and the gases were analyzed as a function of the carbonization temperature, either by gas chromatography or by mass spectroscopy. In

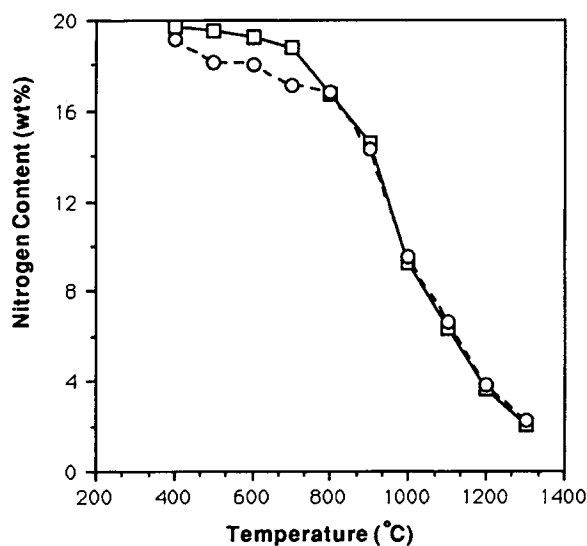


Figure 1 Temperature dependence of nitrogen content in fibers: (□) fiber A; (○) fiber B.

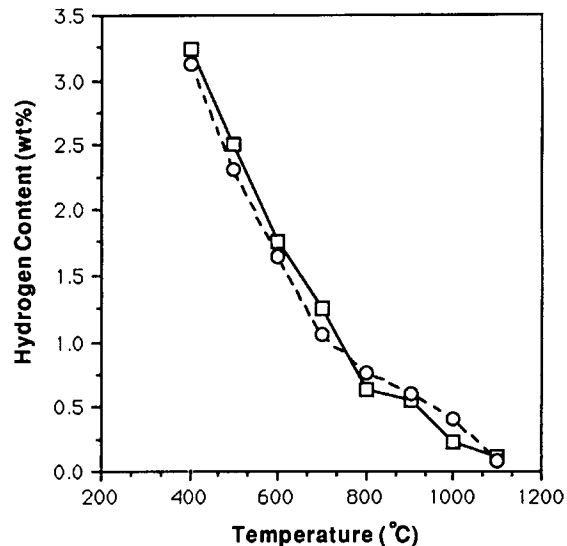


Figure 2 Effect of temperature on hydrogen content in fibers: (□) fiber A; (○) fiber B.

this study, the elemental contents and elemental compositions of stabilized fibers during carbonization are analyzed by elemental analysis. The results are shown in Figures 1–4. During carbonization, the carbon content increases while the oxygen, hydrogen, and nitrogen content decreases.

Figure 1 gives the results of the nitrogen content analysis. The nitrogen content for both samples decreases when the carbonization temperature is raised. In the early stage of carbonization, the ni-

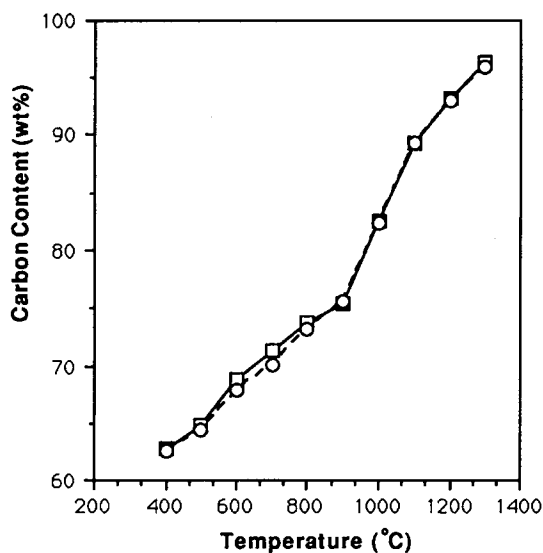


Figure 3 Carbon content for fibers as function of temperature: (□) fiber A; (○) fiber B.

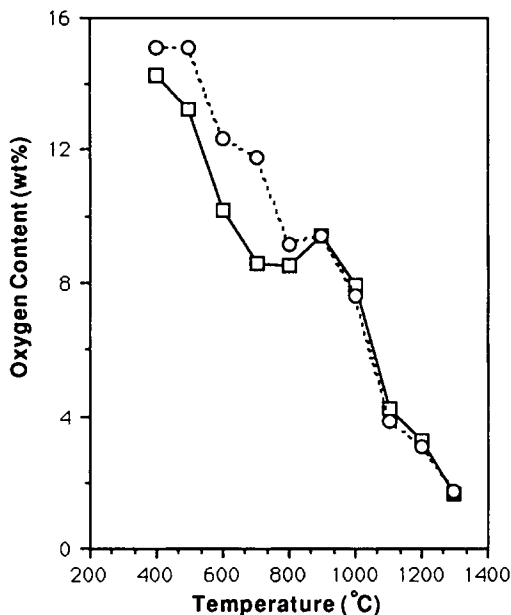


Figure 4 Temperature dependence of oxygen content in fibers: (□) fiber A; (○) fiber B.

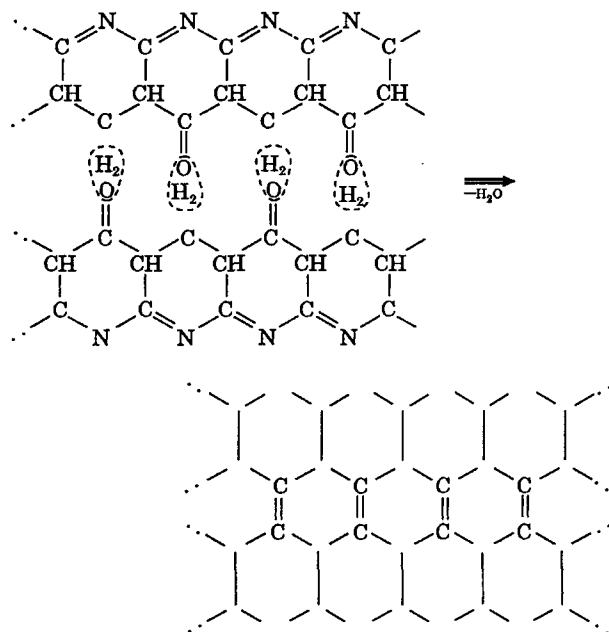
trogen content decreases slightly. After the period of the transition temperature, it decreases rapidly as the carbonization temperature rises. The transition temperature is 700°C for fiber A and 800°C for fiber B. This decrease in nitrogen content is remarkably sharp during carbonization between the transition temperature and 1300°C, showing that the lengthening and broadening of the carbon basal planes occurs rapidly in this temperature range. The transition temperature of fiber B is 100°C lower than that of fiber A. This finding indicates that PAN fiber modified with potassium permanganate will delay the formation of the carbon basal planes. The nitrogen content of the carbon fibers from fiber A, below 700°C carbonization, is higher than that of the carbon fibers developed from fiber B. However, after 800°C carbonization, the carbon fibers from fiber B show a slightly higher nitrogen content when compared to those of fiber A. As a result, fiber A will have more carbon basal planes than will fiber B during carbonization. In addition, the modulus of carbon fibers from fiber A will be higher than that of carbon fibers from fiber B.

As shown in Figure 2, the hydrogen content of carbon fibers from fibers A and B shows a sharp decrease during carbonization, and all hydrogen is lost after 1100°C carbonization. The hydrogen content of carbon fibers developed from fiber A, compared to that of carbonized B fibers, has a similar pattern to that of the nitrogen content. The hydrogen content for fiber A is higher than that for fiber

B before 700°C carbonization. However, the hydrogen content for fiber A is lower than that for fiber B above 800°C. The major chemical reaction products at temperatures ranging from 600° to 1000°C were HCN, H₂, and N₂.²² Whereas HCN is produced by intermolecular cross-linking, H₂ evolves as a result of dehydrogenation. The form of graphitelike ribbons and fibrils in the carbon fibers is due to dehydrogenation and nitrogen elimination.⁴ Thus, the smaller hydrogen content for fiber A during heating between 800 and 1000°C shows that carbon basal planes and fibril formations occur rapidly in this temperature range.

The carbon content of carbon fibers from fibers A and B, as a function of the carbonization temperature, has been plotted in Figure 3. A slight increase in the carbon content during heating from 300 to 800°C can be observed. When the temperature is above 800°C, a higher increase in carbon content occurs. The carbon content for both fibers increases rapidly after 900°C, indicating that the chemical reactions and the formation of carbon basal planes and fibrils occurs very rapidly. The carbon content for fiber A is higher than that for fiber B during the carbonization stage. The carbon content for fiber A is 96.33 wt % and that of fiber B is 96.05 wt % at 1300°C. The higher carbon content indicates that more basal planes were formed for fiber A during carbonization.

As shown in Figure 4, which presents the plots of the oxygen content versus the carbonization temperature for the fibers, the oxygen content is not measured directly, but is calculated by difference. Therefore, this measurement is affected by errors in the carbon, hydrogen, and nitrogen determinations. Starting at a temperature of 400°C, the oxygen content decreases as the temperature increases. Despite this general decreasing pattern, a slight increase in oxygen content is observed between 700 and 900°C for fiber A and between 800 and 900°C for fiber B. With a further increase in carbonization temperature, the oxygen content continues to decrease as the carbonization temperature increases to above 900°C. The oxygen content of carbon fibers developed from fiber A, as compared to those developed from fiber B, are lower from 400 to 700°C, but they are higher when the carbonization temperature is above 800°C. It is known that there is a considerable evolution of H₂O in the early stages of carbonization, 300–500°C. Manocha and Bahl²⁵ suggested that the evolution of H₂O results from the cross-linking condensation reactions between two monomer units of the adjacent ladder polymeric molecular chains such as



In Table II, the oxygen content is 14.7 and 14.0 wt % for fiber A and fiber B during the stabilization stage, respectively. The oxygen content of fiber A is lower than that of fiber B during heating from 400 to 700°C, indicating a significant cross-linking condensation reaction in fiber A. This reaction produces a broadening of the heterocyclic structure, hence, a higher modulus for fiber A carbonized.

The Density, Pore Area, and Preferred Orientation

Figure 5 shows the variation in densities of stabilized fibers during carbonization. Density increases very rapidly below carbonization temperatures of 1000 and 900°C for fibers A and B, respectively. This finding indicates that the aromatization and cross-linking of the heterocyclic rings, as well as the lengthening and broadening of carbon basal planes, led to the repacking of the structure in carbon fibers. However, the density increase was followed by a sharp drop at 1100°C for fiber A and at 1000°C for fiber B. A similar phenomenon has been found by Gibson²⁶ and by Abhiraman et al.²⁷ Gibson observed that a decrease in density for carbon fibers was produced at carbonization temperatures from 1000 to 2000°C. Abhiraman et al. found that an increase in the measured density of carbon fibers occurred below 1200°C, but the density dropped sharply with continued heating. The reason for the drop in apparent density could be the conversion of open pores to closed pores. Consolidation around the pores occurs during the high carbonization temperature.

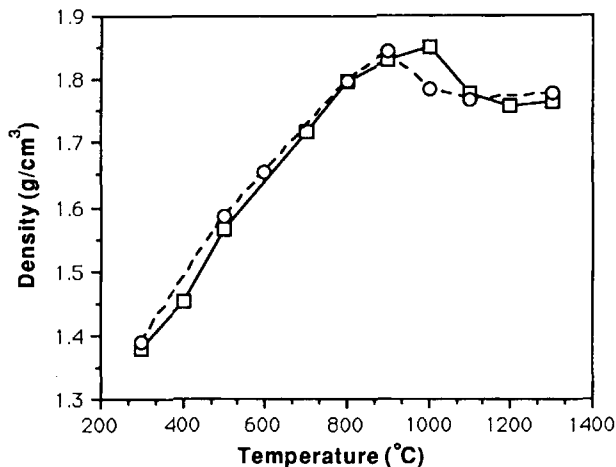


Figure 5 Change in density during carbonization of samples: (□) fiber A; (○) fiber B.

In our early work, a proposed model of a stabilized fiber was built.¹⁵ The stabilized fiber was composed of lamellar-plate-like structure (LPLS) along the fiber axis, as shown in Figure 6. Fibers A and B have the same structure. The spacing is from 100 Å to several hundred Å between two LPLS. The large spacing between two LPLS is one kind of open pore. The lamellar plates could be packed together during the carbonization stage, narrowing the pores. The dimensions of the large open pores decrease when the carbonization temperature is raised during the carbonization stage.

Carbon material contains a complex network of pores of varied shapes and sizes.^{28,29} The shapes include cylinders, rectangular cross sections, and many irregular shapes and constrictions. Because the sizes and shapes are thin, needlelike, and irregular, the small-angle X-ray technique is limited and cannot distinguish between open and closed pores. Therefore, gas and liquid adsorptions of different-sized molecules can offer more information about the variety of surface properties and pore-size distribution.

The pore area of the samples during carbonization were determined by a mercury porosimeter. The progression of the changes in cumulative pore area is plotted as a function of the carbonization temperature in Figure 7. The cumulative pore area of fiber A increased rapidly to a value of 710 m²/g at 900°C, and 449 m²/g at 700°C, suggesting that the fibers were releasing H₂O, HCN, N₂, H₂, CO, and CO₂ and that the reactions led to some narrow, needlelike open pores in the fibers. The cumulative pore area dropped sharply at 1000°C.

When fiber A was carbonized at 1000°C, a higher density (Fig. 5) and a lower cumulative pore area

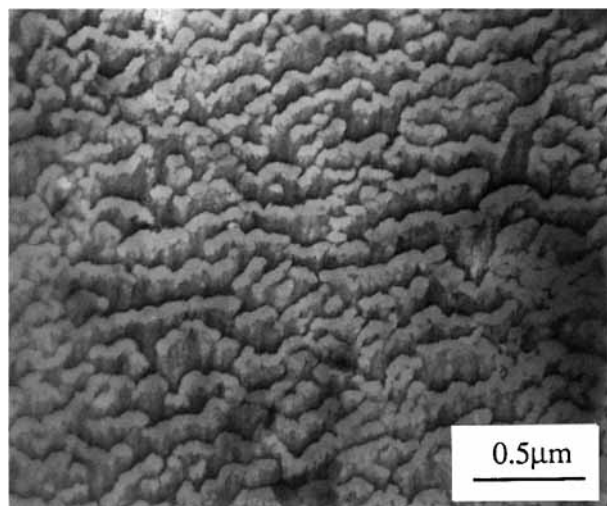


Figure 6 Brightfield image of the inclined section of a stabilized fiber showing the lamellar-plate-like structure (LPLS).

were obtained (Fig. 7). Both findings are consistent with the lengthening and broadening of the carbon basal planes. As a result, the basal planes become closely packed and the structure around the pores is rearranged.

For fiber B, the cumulative pore area decreased sharply during heating from 700 to 1000°C. The cumulative pore area of fiber B decreased below 500°C, that is, at a temperature 200°C lower than that of fiber A. Fiber B had a lower cumulative pore area

than did fiber A during the carbonization stage, indicating that the structure of fiber B was more compact than that of fiber A. Johnson and Tyson³⁰ measured changes in the void diameter by using an X-ray small-angle scattering. They found that an increase in diameter from 0.9 to 2.9 nm occurred with a heating temperature from 1000 to 2400°C, respectively.

The reason the conversion temperature for fiber B was 200°C lower than that of fiber A (Fig. 7) is not apparent at this point. A study of the catalytic graphitization of carbon in 22 kinds of metal powder was made by Oya and Otani.³¹ They found that Mn metal produced large graphitic crystal flakes at an early stage of the catalytic graphitization process. Our findings are consistent with theirs, for Mn metal.

Fiber B was developed from a modified PAN fiber. The Mn catalyzed carbon during the carbonization stage, and the reaction promoted a compacting of the basal planes that led to the conversion of open to closed pores at a lower carbonization temperature. The catalytic reaction not only produced more packing, but also a more orderly arrangement of the basal planes for fiber B. Therefore, the density and the preferred orientation for fiber B were higher than that of fiber A during the final carbonization temperature.

The first paper describing the development of structure in the fibers during the carbonization process was published by Watt et al.²³ They used a tem-

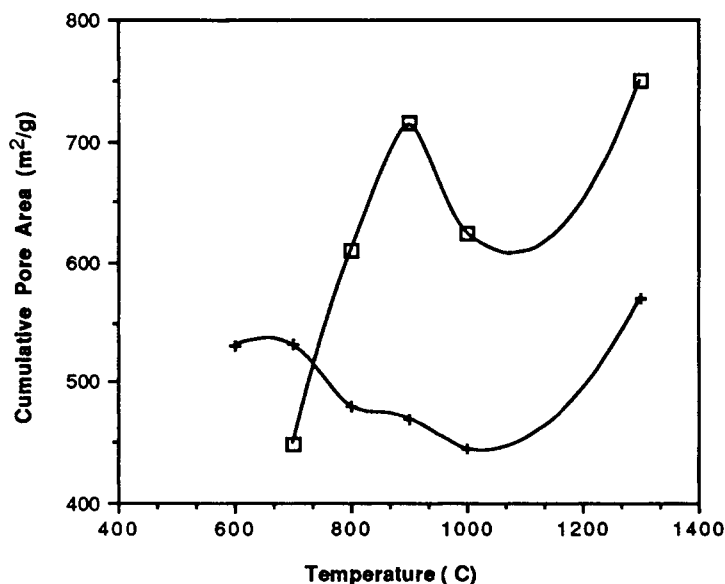


Figure 7 Change in cumulative pore area during carbonization of fibers: (□) fiber A; (+) fiber B.

perature of 320 to 800°C, and found that the preferred orientation of the carbon fibers increased with temperature throughout the range. In our study, the progression of preferred orientation changes of the carbon fibers was plotted as a function of the carbonization temperature (300 to 1300°C), as shown in Figure 8. We observed a similar phenomena in the initial stage of carbonization. However, the preferred orientation of the carbon fibers in our study increased, then, dropped sharply at 1100 and 1000°C for fibers A and B, respectively.

This decrease in the preferred orientation is quite significant. Its pattern parallels the decreases in density that occurred at the same temperatures (Fig. 5). These findings suggest that the broadening of the carbon basal planes could lead to the rearrangement and misorientation of structures along the fiber axis in this temperature range. Above the conversion temperature, 1100 and 1000°C for fibers A and B, respectively, the improvement in preferred orientation is quite significant, indicating that the carbon basal planes become increasingly packed together, yet still remain parallel to the fiber axis throughout the final temperature range.

Watt et al.²³ indicated that as the number of basal planes parallel to the fiber axis increased from 320 to 800°C, the basal planes perpendicular to the fiber axis became broader above a carbonization temperature of 800°C. They also showed that a significant broadening of the basal planes occurred above 1000°C. Therefore, the main reason for the conversion of open to closed pores could be the broadening of the basal planes during carbonization, which could

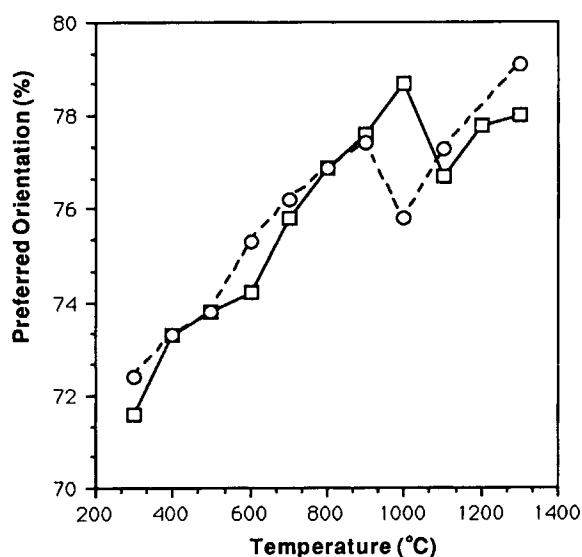


Figure 8 Preferred orientation as a function of carbonization temperature: (□) fiber A; (○) fiber B.

lead to the closing of the surface entrances from open structure.

X-Ray Diffractometer Studies

In carbon fibers, the crystallites are arranged around the longitudinal axis of the fiber with the layer planes. The layer planes are formed by a set of turbostratic stacks of aromatic layers lying approximately parallel to the fiber axis. The structure and microtexture of carbon fibers have been determined by TEM. In a 002 darkfield, the stacks of the basic structural unit (BSU) seen edge-on are imaged as bright domains.^{31,32} Oberlin and Oberlin³³ have measured the thickness and diameter of bright domains, which are replaced by a set of straight and parallel fringes having a length that is the diameter of the BSU.

In our article, the microstructure parameters of two different stabilized fibers during the carbonization stage were studied by X-ray diffraction techniques. An X-ray beam directed perpendicular to the axis produced reflections from the layer planes. The Scherrer equation is used to calculate the values of L_c (stacking height of layer planes) from the width of the 002 reflection. The Bragg equation was used to calculate the d spacing (the distance between the layer planes) from the 002 reflection. Therefore, the mean layer planes in single crystallite could be obtained from L_c/d .

The mean layer planes (L_c/d) as a function of post-heat-treatment temperature are given in Figure 9. The results show the strong effect of the modification process on the PAN fibers and on the mean layer planes of the final carbon fibers. The mean layer planes increase very rapidly during carbonization below 900°C and below 700°C for fiber A and fiber B, respectively. These findings suggest significant aromatization and cross-linking of heterocyclic rings, which leads to the layer planes packing in the fibers. However, the layer plane increase is followed by a sharp drop. Then, at 800 and 1100°C for fibers A and B, respectively, there is a significant increase to 1300°C. This very unusual variation in the mean layer planes of carbon fibers during the carbonization process has not been studied before. However, we have observed this pattern in our work with both the batch carbonization and the continuous carbonization process.³⁴

As the pyrolysis temperature was increased, Watt et al.²³ studied the basal planes of the graphite structure parallel and perpendicular to the fiber axis. They showed that the length parallel to the fiber axis grew much more rapidly than did the breadth

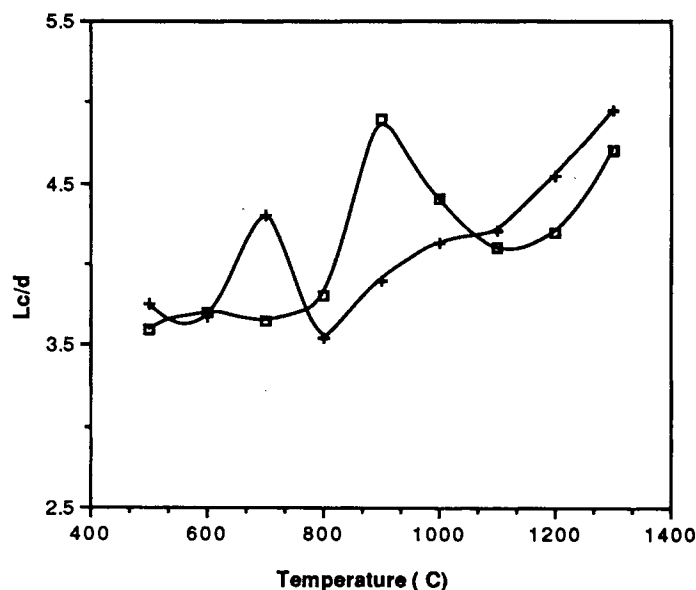


Figure 9 Mean layer planes (Lc/d) as a function of carbonization temperature: (\square) fiber A; (+) fiber B.

normal to the axis in the temperature range of 320 to 800°C. They also showed that the stacking height of the layer planes (Lc) grew from 1.3 nm at 410°C to 1.5 nm at 800°C.

Our study provides more information about the variety in stacking height of the basal planes above a heat-treatment temperature of 800°C. This study shows that the Lc/d for fiber A increases slowly below 800°C. Between 800 and 900°C, the Lc/d for fiber A increases remarkably. This finding indicates that most of the layer planes pack to the incipient layer planes in the developing turbostratic carbon structure. This result may be caused by the broadening of the layer planes perpendicular to the fiber axis.

During the heat-treatment stage from 900 to 1100°C, the mean layer planes suddenly decrease; the density, the cumulative pore area, and the preferred orientation also decrease (see Figs. 5, 7, and 8), which indicates that the cross-linking and broadening of the layer planes are displaced. Some layer planes grow and rearrange around the open pores, resulting in the formation of closed pores. Because some of the crystallites grew around the walls of the pores, there is a decrease in the mean layer planes (Lc/d), the density, and the preferred orientation of carbon fibers in this carbonization stage.

Bennett et al.,³⁵ using a TEM technique, have found that there are large misoriented crystallites present in some walls of the internal flaws of Type

I PAN-based carbon fibers. They reported that the presence of such crystallites has a deleterious effect on fiber strength. We believe that those misoriented crystallites were initially formed during the conversion stage from open to closed pores.

During carbonization above 1100°C for both fibers, the improvement in the growth of oriented crystallites with an increase in heat-treatment temperature is quite significant. There is also an abundant increase in the mean number of layer planes, the preferred orientation, and the density. An overall increase in the mean layer planes shows that the crystallites parallel to the fiber axis are growing and packing much more rapidly than are those surrounding the pores at carbonization temperatures above 1000°C.

For fiber B, developed from modified PAN fiber, the crystallites began to grow around the walls of the pores from 700 to 800°C during carbonization. This phenomenon leads to a decrease in cumulative pore area (Fig. 7). Above this range, more layer planes grow and pack parallel to the fiber axis. Above the carbonization temperature of 1100°C, fiber B has a greater stacking size (Lc) and more layer planes (the higher value of Lc/d) in the crystallite than does fiber A. This finding is due to the catalysis of carbon by Mn that promoted the growth and the close packing of the oriented layer planes. Therefore, the density, the preferred orientation, and the mean layer planes for fiber B are higher than those for fiber A in the final carbonization stage.

The layer planes grow and pack around the walls of open pores. This process leads to the conversion of open pores to closed ones during the carbonization stage. This phenomenon needs to be reconfirmed with the TEM technique that was developed by Bennett et al.,³⁵ in order to provide more information about crystallite growth around the walls of pores.

The Mechanical Properties and Morphology

The results of the influence of heat treatment on the modulus and tensile strength of carbon fibers during the carbonization stage are plotted in Figures 10 and 11. The modulus increased slowly below 500°C and then increased rapidly above this temperature. Below 500°C, the hydrogen content decreased rapidly (Fig. 2), and the carbon content increased slowly (Fig. 3). The oxygen content decreased gradually (Fig. 4), indicating that the main reactions were the evolution of H₂O, CH₄, and CO₂ from the two samples. These reactions promoted a cross-linking of heterocyclic rings, which formed sufficient carbon basal planes to cause a dramatic increase in the modulus and tensile strength.

The modulus and tensile strength for both fibers A and B increased linearly with an increase in temperature above 500°C, as shown in Figures 10 and 11. Raising the temperature above 500°C promoted the formation of longer and broader basal planes, which led to an increase in modulus and tensile strength. Because fiber A had more carbon content in the carbonization stage (Fig. 3), the modulus for

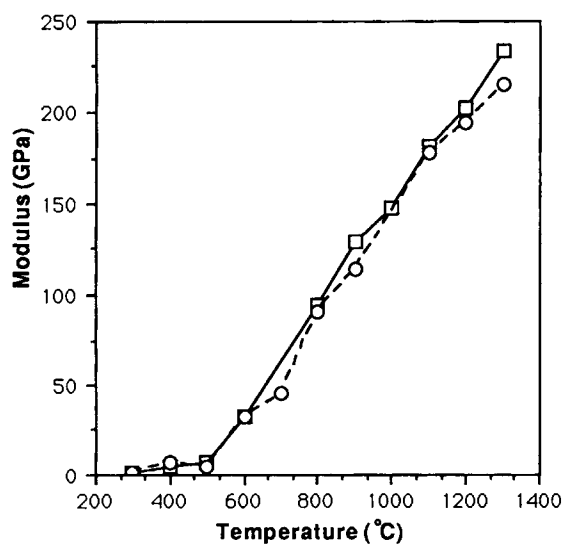


Figure 10 Change in modulus during carbonization of fibers: (□) fiber A; (○) fiber B.

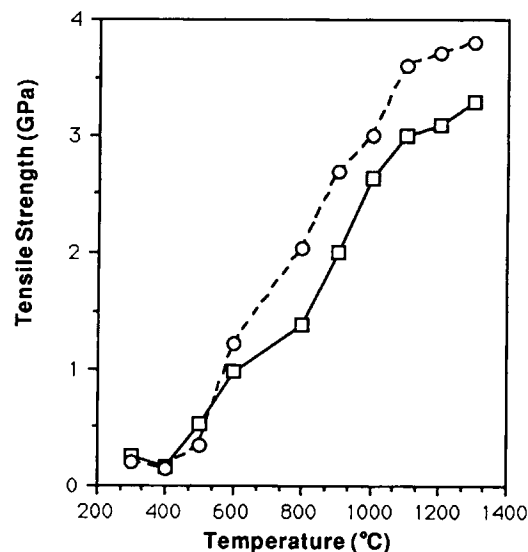


Figure 11 Change in tensile strength during carbonization of fibers: (□) fiber A; (○) fiber B.

fiber A was slightly higher than that for fiber B. However, the carbonized B fiber shows an improvement in tensile strength of 20–40% over that of the carbonized A fiber.

Why do carbonized B fibers have a higher density, a greater stacking size (L_c), more layer planes in the crystallite (L_c/d), a higher preferred orientation, and a higher tensile strength than do carbonized A fibers? These parameter differences suggest strongly that the modification of PAN fibers results in improvements in the final properties of carbon fibers. A possible reason for this process at the molecular level may be that the Mn contained only in fiber B is highly reactive with the carbon because it has an uncompleted d -electron shell.^{37,38} The Mn forms strong chemical bonds with carbon, resulting in a metal carbide. In addition to the powerful bonds between Mn and carbon, another possible process is suspected to be responsible for the tensile strength of the carbonized B fibers. Mn metal has been found to catalyze the formation of graphitic and turbostratic carbons during the heat-treatment stage in experiments conducted by Oya and Otani.³¹

When variation in mean layer planes (Fig. 9) was compared to the relationship between modulus and temperature (Fig. 10), we found that (1) the mean layer planes in fiber A increased at 400–900°C and then suddenly decreased at 900–1100°C. From 900 to 1100°C, fiber A lost 8.15 wt % in nitrogen content (Fig. 1) and increased 53.5 GPa in modulus; (2) the mean layer planes in fiber B increased from 400 to 700°C and then suddenly decreased at 700–800°C.

From 700 to 800°C, fiber B lost 0.25 wt % in nitrogen content and increased 51.6 GPa in modulus.

The mean number of layer planes dropped in the transformational stage (Fig. 9), indicating that the number of basal planes misoriented, relative to the fiber axis, was greater than those oriented to the axis. Because nitrogen loss for fiber A was greater than that for fiber B, the lengthening and broadening of the basal planes in fiber A was quite significant. In fiber B, however, the rearrangement of microstructure occurs at a lower temperature and with less loss of nitrogen, indicating that the rearrangement of the microstructure in the two fibers differs during the final carbonization stage. This difference in basal plane orientation is reflected in different morphologies of the fracture surface in the final carbon fibers.

A scanning electron microscopy (SEM) was used to study the fracture surfaces of the carbonized fibers A and B. A typical fracture surface of carbonized fiber A is shown in Figure 12(a). The microstructure is similar to that of the partially stabilized Courttelle carbon fibers.³⁶ The fracture surfaces of carbonized fiber A have a wraparound basal plane structure in the outer zone and a radial structure in the core. The fracture surface of carbonized fiber B is shown in Figure 12(b); the radial structure is visible only by cross section.

The mode of carbonization of fibers A and B is shown in Figure 13. When fiber A was heated in air for a long time during the stabilization stage, the dimension of the outer zone increased. The stabilization stage for fiber B had no effect on the morphology of the fracture surface for the resulting carbon fibers. The cross section of the resulting carbon fibers from fiber B always had a radial structure.

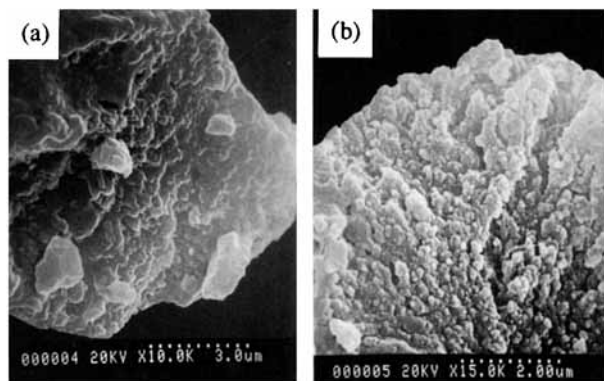


Figure 12 SEM images of fracture surface of the carbon fibers developed from (a) modified PAN fiber and (b) unmodified fiber.

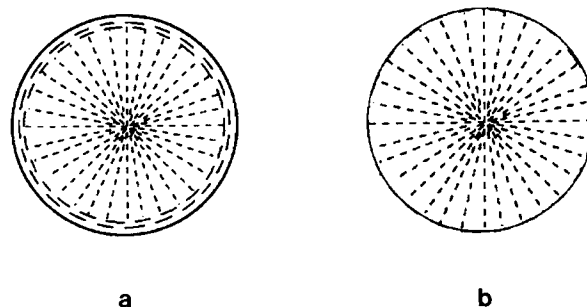


Figure 13 Models of cross sections of the carbon fibers developed from (a) fiber A and from (b) fiber B.

CONCLUSIONS

The modification of PAN fibers during the carbonization process was studied. During carbonization above 1100°C, the carbon fibers developed from modified PAN fibers have a higher density, a higher preferred orientation, and more mean layer planes in crystallite. Because of the Mn-metal-catalyzed formation of graphite during the carbonization stage, the formation temperature of closed pores from open pores in modified fibers was 200°C lower than that for unmodified fibers. The carbonized-modified PAN fibers showed a radial structure on fracture surfaces. The carbon fibers developed from modified PAN fibers showed an improvement in tensile strength of 20–40%.

The author would like to thank Dr. J. Macusar (MIT) for his interest in this work and Mr. P. Chiranairadul for his help in the lab, Ms. Karen Mitzner at MIT for her help in editing this manuscript, and our proofreader Roberta Hoffman. Also, thanks to the National Science Council of the Republic of China for financial support on this study.

REFERENCES

1. T. A. Edison, U. S. Pat. 470,925 (1892).
2. A. Shindo, Rep. Govt. Ind. Res. Inst., Osaka, Japan, No. 317 (1961).
3. W. Johnson, L. N. Philips, and W. Watt, Br. Pat. 1,110,791 (1968).
4. J. B. Donnet and O. P. Bahl, *Encyclopedia Phys. Sci. Tech.*, **2**, 515 (1987).
5. J. Matsui, H. S. Matsuda, and K. Maeda, *J. Ind. Fabrics*, **3**, 43 (1985).
6. W. Watt, L. N. Philips, and W. Johnson, *Engineer (Lond.)*, **221**, 815 (1966).
7. W. Watt and W. Johnson, *Appl. Polym. Symp.*, **9**, 215 (1969).

8. R. B. Mathur et al., *Fibre Sci. Tech.*, **20**, 227 (1984).
9. O. P. Bahl, R. B. Mathur, and T. L. Dhama, *Mater. Sci. Eng.*, **73**, 105 (1985).
10. R. B. Mathur, O. P. Bahl, and K. D. Kundra, *J. Mater. Sci. Lett.*, **5**, 757 (1986).
11. D. E. Cagliostro, *Text. Res. J.*, **50**, 632 (1980).
12. C. H. Lin, H. Y. Ting, and T. H. Ko, in *Proceedings of the 2nd Korea-China Joint Meeting on Textile and Technology*, Seoul, Korea, 1985, p. 108.
13. T. H. Ko, H. Y. Ting, and C. H. Lin, *J. Appl. Polym. Sci.*, **35**, 631 (1988).
14. T. H. Ko and C. H. Lin, *J. Mater. Sci. Lett.*, **7**, 628 (1988).
15. T. H. Ko et al., *J. Appl. Polym. Sci.*, **35**, 863 (1988).
16. T. H. Ko et al., *J. Appl. Polym. Sci.*, **37**, 541 (1989).
17. T. H. Ko, C. H. Lin, and H. Y. Ting, *J. Appl. Polym. Sci.*, **36**, 553 (1989).
18. W. Watt, in *3rd Conference on Industrial Carbons and Graphites*, London, 1971, p. 431.
19. W. Watt and W. Johnson, *Nature*, **257**, 210 (1975).
20. J. R. Bandrup, J. R. Kirby, and L. H. Peebles, *Macromolecules*, **1**, 59 (1968).
21. O. P. Bahl and L. M. Manocha, *Carbon*, **12**, 417 (1974).
22. W. Watt and J. Green, in *Proceedings of the International Conference on Carbon Fibers, Their Composites and Applications*, Plastic Institute, London, 1971, p. 23.
23. W. Watt, D. J. Johnson, and E. Parker, in *Proceedings of the 2nd International Plastics Conference on Carbon Fibres*, Plastics Institute, London, 1974, p. 3.
24. D. A. Brandreth, W. M. Riggs, and R. E. Johnson, *Nature Phys. Sci.*, **236**, 10 (1972).
25. L. M. Manocha and O. P. Bahl, *Fibre Sci. Technol.*, **13**, 199 (1980).
26. D. W. Gibson, *18th Int. SAMPE Symp.*, **18**, 165 (1973).
27. A. S. Abhiraman et al., *J. Mater. Sci.*, **22**, 3864 (1987).
28. P. H. Emmett, *Chem. Rev.*, **43**, 69 (1948).
29. E. O. Wing and S. B. Smith, *J. Phys. Colloid Chem.*, **55**, 27 (1951).
30. D. J. Johnson and C. N. Tyson, *J. Phys. D Appl. Phys.*, **3**, 526 (1970).
31. A. Oya and S. Otani, *Carbon*, **17**, 131 (1979).
32. A. Oberlin, *Carbon*, **17**, 7 (1979).
33. A. Oberlin and M. Oberlin, *J. Microsc.*, **132**, 353 (1983).
34. T. H. Ko, unpublished data, 1989.
35. S. C. Bennett, D. J. Johnson, and W. Johnson, *J. Mater. Sci.*, **18**, 3337 (1983).
36. R. H. Knibbs, *J. Microsc.*, **94**, 273 (1971).
37. M. Wakastuki, *Tanso*, **57**, 204 (1969).
38. M. Wakastuki, K. Ichinose, and T. Aoki, *Toshiba Rev.*, **23**, 785, (1968).

Received August 13, 1990

Accepted November 27, 1990